JMEPEG (2010) 19:287–293
DOI: 10.1007/s11665-009-9456-0

1059-9495/$19.00

Microstructure-Related Properties of Some Novel Reinforcement Bar Steel

B.K. Panigrahi

(Submitted August 2, 2008; in revised form April 7, 2009)

Mechanical properties particularly Charpy impact toughness of two low-carbon [(a) 0.11% phosphorus and (b) 0.009% niobium] thermomechanically treated reinforcing bar steels were investigated. The phosphorus and niobium steels showed tensile to yield strength ratio of 1.25 and 1.19, ductile-brittle transition temperature of 223 K and below 193 K at yield strength levels of 428 and 472 MPa, respectively. The improved toughness of phosphorus steel is attributed to a mixed transformation microstructure comprising low-carbon bainite and fine polygonal ferrite. Lowest ductile-brittle transition temperature was observed in the niobium steel due to overall fineness of microstructure consisting mainly of low-carbon bainite, acicular ferrite, and polygonal ferrite.

Keywords impact behavior, microstructure, P/Nb-alloyed rebar, tensile properties

1. Introduction

Considering that large areas of Indian subcontinent are situated in earthquake prone zones (Ref 1), effort has been directed in recent years to develop steels that will suit construction in these regions. In an earthquake, lateral loads are generated, the magnitude of which can be over 10 times that of other type of design lateral load, i.e., wind. Due to this lateral load, besides constant vertical load exerted by a tall structure, steels used in structures are expected to exhibit sufficient strength, higher tensile to yield strength ratio (UTS/YS) (Ref 2, 3), and energy dissipation capacity (i.e., elevated internal friction and good elongation). Over and above, the toughness (Ref 4) is also an important property to resist brittle fracture particularly in subzero climatic condition. These properties can be achieved at low cost by thermomechanical treatment (TMT) (Ref 5) in a rolling mill. Rebars being a mass-produced constructional material, its cost should be low for large-scale usage. Generally, carbon-manganese rebar in semi-killed or killed variety is used. Higher carbon and manganese in rebar have adverse effect on weldability and impact toughness. Therefore, to maintain these properties at acceptance levels, various possibilities to lower carbon and manganese which impart strengthening were explored. These are alloying with phosphorus, higher than that normally found in mild steel, microalloying by vanadium/niobium, and alloying with chromium. The latter (chromium rebar) is used at very high strength level (yield stress: 600 MPa, min.) (Ref 6).

Previous studies on low-carbon corrosion-resistant TMT rebar have shown that besides improving corrosion resistance, phosphorus contributes toward strength, without adverse effect on ductility when carbon is low (Ref 5). In phosphorus-bearing low-carbon steels, the atoms of phosphorus are in solid solution of α-iron causing the strengthening effect of ferrite without adverse effect on ductility. Since the Gibbs free energy for grain boundary segregation of phosphorus (−49 kJ/mol) is higher than carbon (−72 kJ/mol) at 773 K, which is in the neighborhood of temperature of equalization for phosphorus-bearing TMT rebar, carbon preferentially segregates at the grain boundary displacing phosphorus (Ref 7, 8).

Due to technoeconomic consideration, vanadium microalloyed rebar and titanium microalloyed rebar were not produced substantially. The former (vanadium rebar) requires higher quantity of ferrovanadium addition to achieve equivalent strength, and the latter (titanium rebar) must be produced as killed steel. Therefore, microalloying with niobium in semi-killed steel has been used. Tables 1, 2, and 3 show composition, process parameters, and mechanical properties and microstructure of some semikilled rebar steels, respectively (Ref 5, 6, 9).

To lower the cost of steel without adverse effect on mechanical properties, (a) higher phosphorus (0.11 wt.%) and (b) low-niobium (0.009 wt.%) rebars have been produced. In this article, the microstructure-related properties particularly the Charpy impact toughness of these rebars have been highlighted.

2. Materials and Methods

The steel for reinforcing bar was produced in a 250 T twin hearth furnace, and cast as 9000 kg ingots. The ingots were rolled to 325 × 325 mm blooms and then to billets of size 105 × 105 mm. The billets were reheated at 1453 to 1473 K. The processing of billets to TMT rebar of diameter 32 mm was done in a continuous bar mill having roughing, intermediate, and finishing stands followed by a cooling unit. From the

B.K. Panigrahi was formerly with Research and Development Centre for Iron and Steel, Steel Authority of India Limited.

B. K. Panigrahi, Research and Development Centre for Iron and Steel, Steel Authority of India Limited, Ranchi 834002, India and Gandhi Road, Contai, West Bengal 721401, India. Contact e-mail: dr.bkpanigrahi1948@gmail.com.

Table 1 Composition (wt.%) of some semikilled rebar steels

Steel	C	Mn	Si	S	P	Nb	V	Cu	Cr	Ref
C-Mn	0.20	1.2	0.05	0.03	0.02	···	···	···	···	9
C-Mn-Nb	0.21	1.0	0.06	0.036	0.022	0.02	···	···	···	9
C-Mn-V	0.25	1.27	0.03	0.03	0.02	···	0.05	···	···	9
C-Mn-Cu-P	0.15	0.9	0.03	0.02	0.09	···	···	0.30	···	5
C-Mn-Cu-Cr	0.14	0.9	0.02	0.02	0.02	···	···	0.34	0.52	5
C-Mn-Cr	0.25	1.42	0.05	0.02	0.02	···	···	···	0.54	9

Table 2 Processing parameters of some semikilled rebar steels

Steel	Diameter of rebar, 10^{-3} m	Reheating temperature, K	Finish rolling temperature, K	Rolling speed, m/s	Cooling rate, K/s	Equalisation temperature, K	Ref
C-Mn	32-45	1453-1473	1223-1273	6-8	200-250	793-853	9
C-Mn-Nb	32-45	1453-1473	1273-1323	6-8	200-250	813-873	9
C-Mn-V	32-45	1453-1473	1273-1323	6-8	200-250	813-873	9
C-Mn-Cu-P	32-36	1453-1473	1223-1273	6-8	200-250	773-823	5
C-Mn-Cu-Cr	32-36	1453-1473	1223-1273	6-8	200-250	773-823	5
C-Mn-Cr	32	1453-1473	1223-1273	6-8	200-250	773-823	6

Table 3 Tensile properties and microstructure of some semikilled rebar steels

Steel	Yield stress, MPa (min.)	UTS, MPa (min.)	Elongation, % (min.)	Microstructure		Ref
				Rim	Core	
C-Mn	415	485	14.5	Tempered martensite	Ferrite + Pearlite	9
C-Mn-Nb	415	485	14.5	Tempered martensite	Ferrite + Pearlite	9
C-Mn-V	415	485	14.5	Tempered martensite	Ferrite + Pearlite	9
C-Mn-Cu-P	500	545	12	Tempered martensite	Ferrite + Pearlite	5
C-Mn-Cu-Cr	500	545	12	Tempered martensite	Ferrite + Pearlite + Bainite + Carbide	5
C-Mn-Cr	600	660	10	Tempered martensite	Ferrite + Bainite	6

finishing stand, the bar passed through this cooling unit in which pressurized water is circulated on the bar to chill the bar surface at 180 to 200 K/s, immediately forming a rim of lath martensite (M), while the core still remains austenitic (A). On emergence from the cooling unit, the temperature of the bar reaches a steady value (equalization temperature) due to transfer of heat from the core to the rim, and the martensite of rim is tempered. The core finally transforms to a mixed microstructure comprising ferrite (F) of varying morphologies, pearlite/carbide (P)/bainite (B). The schematic of the process is shown in Fig. 1. The rolling speed and finish rolling temperature was 6 to 8 m/s and 1223 to 1273 K, respectively, and the equalization temperature was 833 to 873 K. The finish rolling temperature and the temperature of equalization, after the bar leaves the cooling unit, play dominant role in controlling the microstructure and mechanical properties of the rebar (Ref 5, 9).

Transverse specimens for metallography were machined from the rebar and polished for microstructural investigation after etching in 2% nital. Vickers microhardness of rim and core regions was measured with a load of 50×10^{-3} kg. Tensile test was conducted using duplicate unmachined rebar in accordance with ASTM A 370 Standard (Ref 10) in a 60 kN servohydraulic testing machine. In the tensile test, a gage length of $5.65\sqrt{A}$

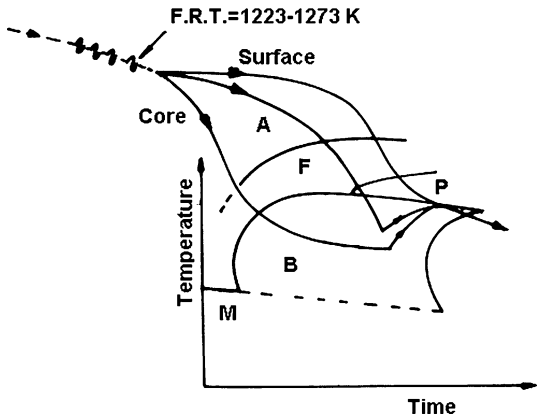

Fig. 1 Schematic of CCT diagram of a TMT rebar (A = austenite; F = ferrite, P = pearlite/carbide; B = bainite; M = lath martensite)

was used, where A is the effective cross sectional area of the rebar and is given by: $M/L\rho$; M is the mass of rebar in 10^{-3} kg, L is the length of rebar in 10^{-2} m, and ρ is the density of steel in 10^3 kg/m^3. The test was done at a cross head speed of 50×10^{-3} m/60 s. Charpy impact toughness was evaluated

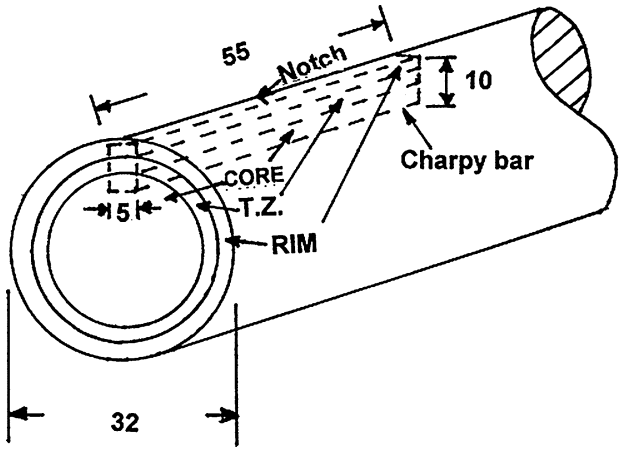

Fig. 2 Location of Charpy specimen in the rebar (TZ = transition zone)

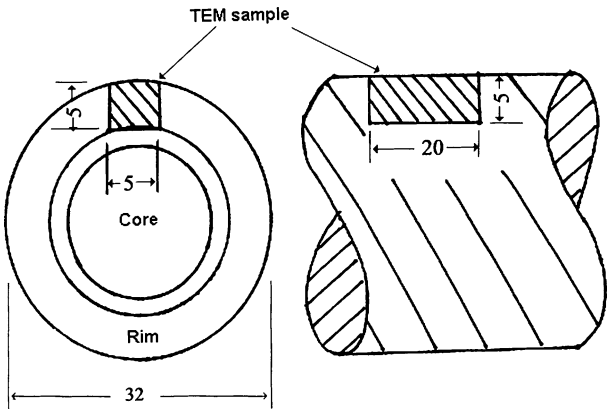

Fig. 3 Location of TEM rod sample in the TMT rebar

using longitudinal specimens of size $5 \times 10 \times 55 \times 10^{-3}$ m machined from the location shown in Fig. 2 to preserve the rim as far as possible, and tested at 298, 273, 253, 233, 213, and 193 K in accordance with ASTM E 23 standard (Ref 11). For preparation of transmission electron microscopic (TEM) specimens, sample of size $5 \times 5 \times 20 \times 10^{-3}$ m was cut from the location shown in Fig. 3. From this sample, 0.5×10^{-3} m thick disc was cut by a thin disc cutter. The disc was further reduced mechanically to 0.1×10^{-3} m thick foil and electrolytically thinned in a twin jet polisher using a solution of 5% perchloric acid and 95% glacial acetic acid at 293 K. The operating voltage was 60 V. Foils were observed at 150 keV.

3. Results

3.1 Chemical Composition

The chemical composition of the experimental and standard steels is given in Table 4. The carbon and manganese in the TMT rebar have been brought down by about 50% with respect to conventional level of 0.20 and 1.20%, respectively. Although it is a solid solution strengthener and a hardenability enhancing element, silicon was kept low to improve the tonnage yield of steel. The required hardenability was ensured through phosphorus (Ref 12) or niobium (Ref 13, 14).

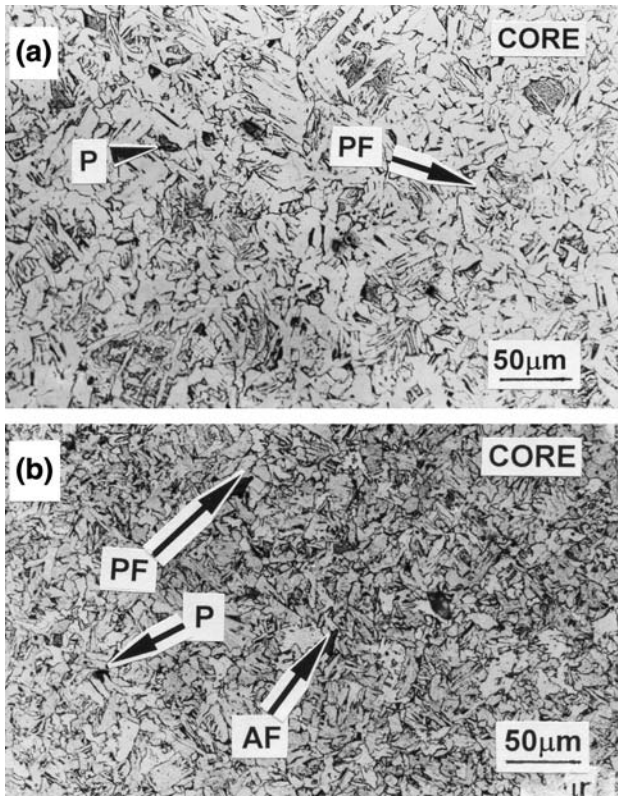

Fig. 4 Optical microstructures of core regions: (a) phosphorus steel and (b) niobium steel (PF = polygonal ferrite; P = pearlite/carbide; AF = acicular ferrite)

Table 4 Typical chemical composition of experimental rebar steels and relevant standards

Elements, wt.%	Experimental steels		
	P steel	Nb steel	C-Mn steel
C	0.077	0.095	0.21
Mn	0.59	0.56	1.14
Si	0.03	0.06	0.05
S	0.023	0.017	0.029
P	0.11	0.019	0.021
Nb	···	0.009	···
Al	0.017	0.0045	···
N	72 ppm	68 ppm	···

Elements, wt.%	Relevant standards		
	IS 1786-2008	ASTM A 706-96	AUS 4671-2002
C	0.30 max	0.30 max	0.22 max
P	···	0.035 max	0.050 max
S	···	0.035 max	0.050 max

3.2 Microstructure of the Rim

The optical microstructures of the core and rim regions are shown in Fig. 4 and 5 for phosphorus and niobium steels, respectively. The rim which is ~4 mm thick depicts primarily low-carbon bainite (LCB) (Ref 15) in both phosphorus and niobium steels. A typical bright field TEM image of LCB is

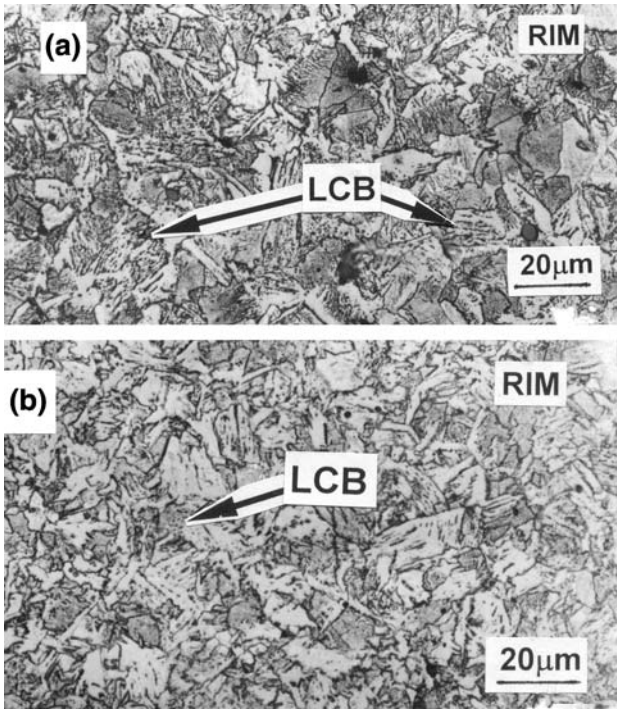

Fig. 5 Optical microstructures of rim regions: (a) phosphorus steel and (b) niobium steel (LCB = low-carbon bainite)

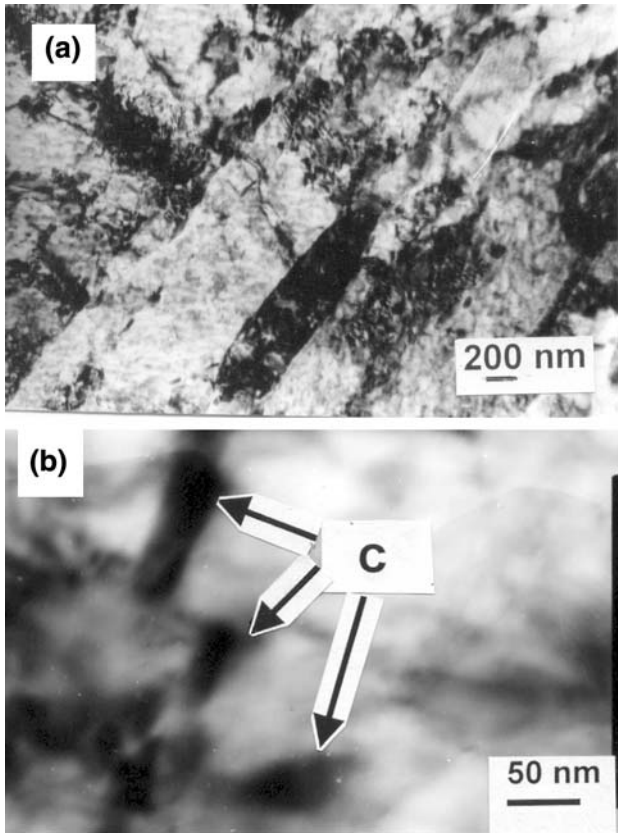

Fig. 6 Bright field TEM image of rim in (a) phosphorus steel and (b) niobium steel (C = carbide)

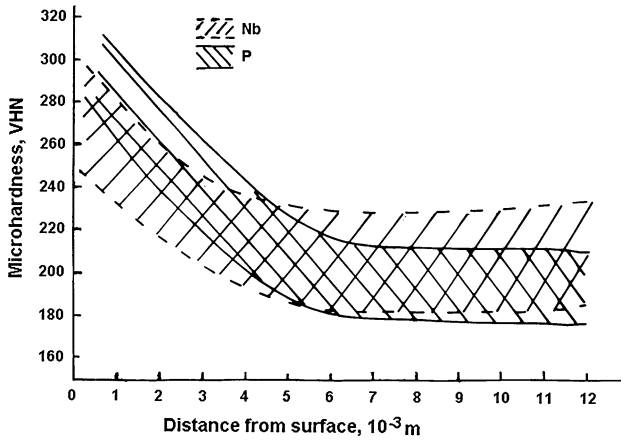

Fig. 7 Variation of microhardness across rim and core of TMT rebar

shown in Fig. 6(a) for phosphorus steel and in Fig. 6(b) for niobium steel. The bainite, which has high dislocation density, is associated with interlath and intralath carbides (cementite) some of which are aligned in the direction of lath axis (Fig. 6a). The rim of niobium steel was literally free from niobium carbonitride precipitates, though carbides (C) were present in the bainitic ferrite. The presence of LCB in TMT rebar can be explained as follows. Due to low carbon and manganese content, the nose of CCT diagram was close to the temperature axis, i.e., shifted leftward, and the time available for martensite rim development was short (Fig. 1). In view of this, the martensite rim was not formed in the prevailing conditions of processing. However, according to literature, martensite (Ref 16) with small amount of retained austenite (Ref 17) can form on quenching this low-carbon steel in water, since solubility of carbon in α-iron at about 323 K is 1 to 2×10^{-4} wt.% (Ref 18). The average microhardness (Fig. 7) of the rim at a distance of 1 mm beneath the surface of TMT rebar in phosphorus and niobium steel was 283 and 256 VHN, respectively which is similar to the hardness of bainite (~300 VHN) (Ref 19) and was quite lower than the hardness of low-carbon-tempered martensite (400 VHN) (Ref 16).

3.3 Microstructure of Transition Zone and Core

The transition zone (Fig. 2) which was about 2 mm thick experienced cooling rates that favored transformation to bainite. The core showed primarily ferrite with pearlite/carbide. The ferrite has two morphologies, namely polygonal (P and Nb steel) or equiaxed type and nonpolygonal (Nb steel) or acicular type. The polygonal ferrite grains are less finer (12.2×10^{-3} m) in phosphorus steel than in niobium steel (8.5×10^{-3} m), and consequently the core hardness of niobium steel was higher (210 VHN) compared to phosphorus steel (193 VHN).

3.4 Tensile Properties

The tensile properties of the experimental phosphorus and niobium steels and a C-Mn steel are given in Table 5 together with those by ASTM A 706 (Ref 2) and IS 1786 standards (Ref 20). The elongation of phosphorus steel was higher (25%) than niobium steel (18%) due to its relatively lower strength. Presence of different microstructural constituents produced good combination of yield strength, YS (428/472 MPa), tensile strength, UTS (539/564 MPa), elongation (25/18%), and tensile to yield strength ratio (1.25 and 1.19) in phosphorus and

niobium steels, respectively. The UTS/YS ratio of niobium steel was relatively lower (1.19) due to finer microstructure of the core region that raised its overall yield strength. This is because yield strength of TMT rebar with composite microstructure comprising rim, transition zone, and core is given by the law of mixture:

$$\begin{aligned}\text{YS of rebar} = {} & \%\text{ area of rim} \times \text{YS of rim} \\ & + \%\text{ area of TZ} \times \text{YS of TZ} \\ & + \%\text{ area of core} \times \text{YS of core}\end{aligned} \quad \text{(Eq 1)}$$

A finer microstructure raises YS by Hull-Petch relationship, whereas the UTS is mainly influenced by solid solution strengthening element such as phosphorus and volume fraction of pearlite (Ref 21). A higher UTS/YS ratio is essential for construction, and the desired UTS/YS ratio varies from 1.15 to 1.40 (Ref 2, 3). The strengthening in the composite (mixed) microstructure of TMT bar is due to a combined effect of operative mechanisms in as-rolled ferrite-pearlite and quenched and tempered steels which are mainly grain size and lath size effects, solid solution hardening, and transformation strengthening. The elongation is influenced by microstructure and strength of the steel. Absence of coarser pearlitic colony and a predominantly ferritic core structure in this low-carbon steel resulted in good elongation.

Table 5 Typical tensile properties of experimental rebar steels compared with relevant standards

	Experimental steels		
	P steel	Nb steel	C-Mn steel
Yield stress, MPa	428	472	463
UTS, MPa	539	564	594
UTS/YS	1.25	1.19	1.28
Total elongation, %	25.0	18.0	20.0

	Relevant standards		
	IS 1786-2008	ASTM A 706-96	AUS 4671-2002
Yield stress, MPa	415 min.	420-540	500-600
UTS, MPa	485 min.	550 min.	···
UTS/YS	···	1.25 min	1.15-1.40
Total elongation, %	14.5 min.	12 min.	10 min.

3.5 Charpy Impact Toughness

Figure 8 shows the variation of Charpy absorbed energy with temperature of the three rebars under evaluation. The decrease of toughness on lowering the temperature from RT (298 K) to 253 K was small. Even at 253 K, the Charpy impact energy was quite high, namely 82 and 120 J for phosphorus and niobium steels, respectively, compared to 45 J for C-Mn steel. The ductile-brittle transition temperatures (DBTT) calculated by 50% maximum energy criterion (Ref 22) are 223 K, below 193 K, and 248 K for phosphorus, niobium, and C-Mn steels, respectively.

4. Discussion

4.1 Toughness of Phosphorus Steel

High fracture toughness is greatly desired for construction in seismic areas, particularly where ambient temperature is low, to

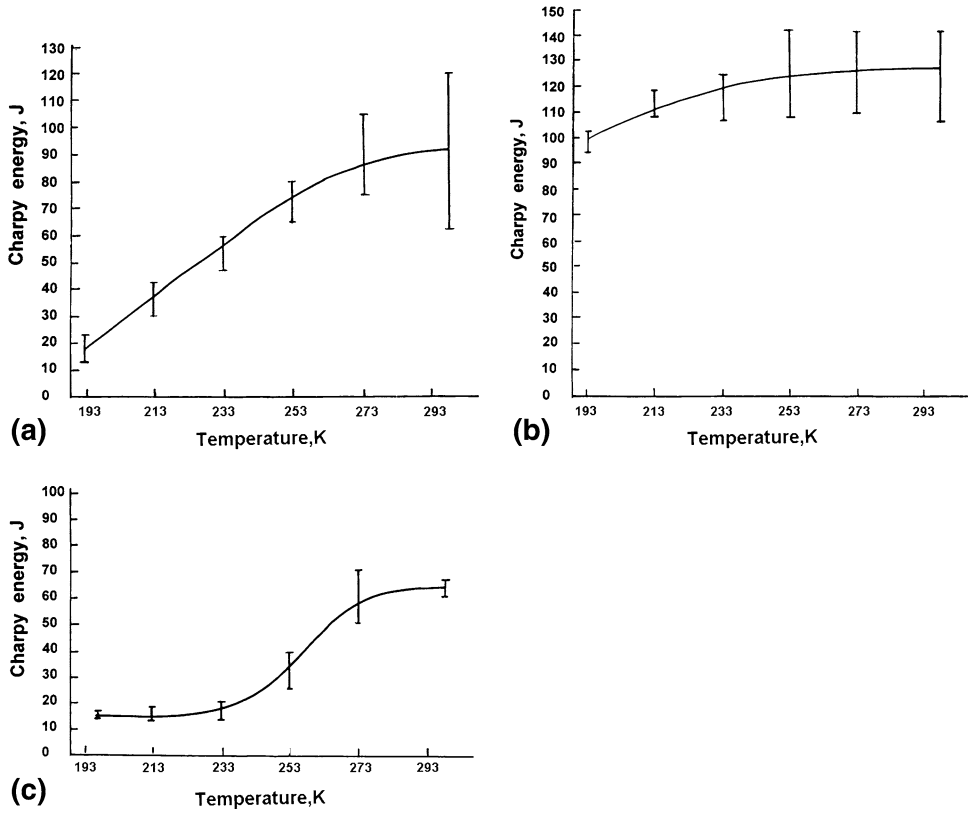

Fig. 8 Subsize Charpy energy vs. temperature curves of (a) phosphorus steel; (b) niobium steel; and (c) carbon-manganese steel

avoid brittle fracture. In this study, the observed subzero toughness of phosphorus steel is similar to a killed titanium microalloyed (C 0.30, Mn 1.14, Si 1.24, S 0.029, P 0.026, Ti 0.036 wt.%) reinforcing hot-rolled bar steel: 25 to 32 mm diameter with fine ferrite-pearlite structure and having Charpy absorbed energy of 73×10^4 J/m^2 at 213 K measured using full-size Charpy specimens (Ref 23). Due to presence of different microstructural constituents ahead of notch, a crack propagates through a variety of microstructures and is hindered at numerous boundaries of bainitic ferrite laths and polygonal ferrite grains (Ref 24, 25) as a result of which DBTT was lowered. Low percentage of carbon and manganese in this steel had also played a key role in lowering the DBTT (Ref 5, 26).

4.2 Toughness of Niobium Steel

Niobium addition in steel increases the yield strength by grain refinement and precipitation strengthening (Ref 21). The former effect improves the toughness. The DBTT of niobium steel was the lowest (below 193 K). In a low-carbon steel, niobium promotes transformation to acicular ferrite due to segregation of solute niobium to the austenite/ferrite boundary (Ref 27, 28) as well as increases bainitic hardenability (Ref 13, 29), resulting in a mixed microstructure. In a mixed microstructure, though there is tendency of brittle fracture initiation in the coarser polygonal ferrite grains because of strain concentration, the polygonal ferrite grains in niobium steel were finer than phosphorus steel resulting in lowest DBTT because DBTT is related to ferrite grain size (Ref 21) as follows:

$$\beta T = \ln \beta - \ln C - \ln d^{-1/2}, \quad \text{(Eq 2)}$$

where β and C are constants, T is the DBTT, and d is the grain size.

The Nb(CN) precipitates, if formed, can lower the toughness. The approximate expression for the solubility product of Nb(CN) in austenite is given by (Ref 30)

$$\log_{10}[\text{wt.\%Nb}] \cdot [\text{wt.\%C} + 12/14\ \text{wt.\% N}] = -6770/T + 2.26 \quad \text{(Eq 3)}$$

where T is the solution temperature of niobium carbonitride in K. The solution temperature of niobium carbonitride in the present steel is about 1273 K. On reheating billets above 1273 K, niobium carbonitrides are dissolved in austenite. Under normal cooling condition, on lowering the temperature below solution temperature of niobium carbonitride, reprecipitation is expected. Since the finish rolling temperature of the bar was about 1273 K, carbonitride could not have precipitated before the bar entered the water cooling unit. Inside the cooling chamber, due to high rate of cooling, the diffusion rates are adversely affected, and the precipitation of Nb(CN) was insignificant in rim, though fine Nb(CN) can form in the core of rebar.

5. Conclusions

The results of two low-carbon constructional TMT reinforcing bar steels containing 0.11% phosphorus and 0.009% niobium are summarized below:

1. Both the steels have good combination of yield strength (P steel: 428 MPa, Nb steel: 472 MPa), tensile strength (P steel: 539 MPa, Nb steel: 564 MPa), and elongation (P steel: 25%, Nb steel: 18%).
2. The phosphorus and niobium steels with UTS/YS ratio 1.25 and 1.19 exhibited DBTT of 223 K and below 193 K, respectively.
3. Transformation to a mixed microstructure comprising low-carbon bainite and finer polygonal/acicular ferrite was primarily responsible for lower DBTT in these steels.

Acknowledgments

Thanks to the management of Steel Authority of India Limited, Bhilai Steel Plant and R&D Center for Iron and Steel, Ranchi where the work was carried out.

References

1. R. Van der Voo, W. Spakman, and H. Bijwaard, Tethyan Subducted Slabs Under India, *Earth Planet. Sci. Lett.*, 1999, **171**(1), p 7–20
2. "Standard Specification for High Strength Low Alloy Structural Steel; Standard Specification for low Alloy Steel Deformed Bars for Concrete Reinforcement," *Annual Book of ASTM Standards*, Vol 01.04, American Society of Testing Materials, West Conshohcken, PA, 1996, p 148–149, 344–348
3. "Reinforcing Steel Materials," Clause 7.2, *Australian Standard*, 2002
4. H. Shimaoka, K. Sawamura, and T. Okamoto, New Construction Materials for Social Infrastructures, *NKK Tech. Rev.*, 2003, **88**, p 88–99
5. B.K. Panigrahi and S.K. Jain, Impact Toughness of High Strength Low Alloy TMT Reinforcement Rebar, *Bull. Mater. Sci.*, 2002, **25**(4), p 319–323
6. B.K. Panigrahi, Relationships of Microstructures and Mechanical Properties of a Fe/Mn/Cr Rock Bolt Reinforcing Steel, *J. Mater. Eng. Perform.*, manuscript ID JMEP-08-12-1085, submitted 07 December 2008 (under review)
7. H.J. Grabke, Effects of Impurities in Steels on Mechanical Properties and Corrosion Behaviour, *Steel Res.*, 1987, **58**, p 477–482
8. B.K. Panigrahi, S. Srikanth, and G. Sahoo, Effect of Alloying Elements on Tensile Properties, Microstructure, and Corrosion Resistance of Reinforcing Bar Steel, *J. Mater. Eng. Perfom.*, 2008. doi:10.1007/s11665-008-9336-z
9. B.K. Panigrahi, Unpublished Results, R&D Center for Iron and Steel, Steel Authority of India Ltd., Ranchi, India, 2008
10. "Standard Test Methods for Mechanical Testing of Steel Products, Methods for Testing Steel Reinforcement Bars," *Annual Book of ASTM Standards*, Vol 03.01, ASTM, West Conshohocken, PA, 1995, p 182
11. "Standard Test Methods for Notched Bar Impact Testing of Metallic Materials," *Annual Book of ASTM Standards*, Vol 03.01, American Society of Testing Materials, West Conshohocken, PA, 2005, p 160–186
12. D.J. Naylor and W.T. Cook, Heat Treated Engineering Steels, in *Materials Science and Technology*, Vol. 7, R.W. Cahn, P. Hassen, and E.J. Kramer, Ed., VCH Publishers, New York, 1992, p 433–488
13. K. Easterling, *Introduction to Physical Metallurgy of Welding*, Butterworths Publishers, London, 1983, p 48–103
14. A.J. DeArdo, J.M. Gray, and L. Meyer, Fundamental Metallurgy of Niobium Steel, in *Niobium*, H. Stuart, Ed., AIME, Warrendale, PA, 1984, p 685–759
15. B.L. Bramfitt and J.G. Speer, A Perspective on the Morphology of Bainite, *Metall. Trans.*, 1990, **21A**(4), p 817–829
16. D.S. Clark and W.S. Varney, *Physical Metallurgy for Engineers*, East West Press, New Delhi, 1968, p 142–242 (East West Edition)
17. E. Houdremont, *Handbuch der Sonderstahlkunde (Handbook of Special Steels)*, 3rd ed., Springer Verlag, Berlin, 1956, p 157–1449 (in German)
18. E. Hornbogen, Physical Metallurgy of Steels, in *Physical Metallurgy*, R.W. Cahn, Ed., North Holland, Amsterdam, 1970, p 589–653
19. I.B. Timokhina, P.D. Hodgson, and E.V. Pereloma, Effect of Deformation Schedule on the Microstructure and Mechanical Properties of a

Thermomechanically Processed C-Mn-Si Transformation Induced Plasticity Steel, *Metall. Trans.*, 2003, **34A**(8), p 1599–1609
20. "Specification for High Strength Deformed Steel Bars and Wires for Concrete Reinforcement," *Indian standards IS 1786*, Bureau of Indian Standards, New Delhi, 2008, p 1–10
21. W.C. Leslie, *The Physical Metallurgy of Steels*, Chapter V, VI, Hemisphere Publishing, New York, 1981
22. W. Dahl, Mechanical Properties, *Steel*, Vol I, Springer Verlag and Verlag Stahl Eisen, Dusseldorf, 1992, p 203–378
23. V.A. Kharchenko, K. Safonova, A.I. Ivanov, I.V. Savchenko, and T.A. Ivleva, Effect of Mn and Ti on Cold Resistance of Reinforcing Steel, *Russ. Metall. (Metally)*, 1987, **5**, p 158–160
24. A. Galibois, M.R. Krishnadev, and A. Dubey, Control of Grain Size and Substructure in Plain Carbon and High Strength Low Alloy Steels—the Problem and the Prospect, *Metall. Trans.*, 1979, **10A**(8), p 985–995
25. D.V. Edmonds and R.C. Cochrane, Structure-Property Relationships in Bainitic Steels, *Metall. Trans.*, 1990, **21A**(6), p 1527–1540
26. L. Pauling, *The Nature of the Chemical Bonds*, Cornell University Press, Ithaca, NY, 1960
27. C.I. Garcia, Transformation Strengthening of Microalloyed Steels, *Microalloying '95*, M. Korchynski, Ed., June 11-14, 1995 (Pittsburgh, PA), ISS-AIME, Warrendale, PA, 1995, p 365–375
28. C. Li, Study of Low Carbon Steel, *Steel Times Int.*, 2001, **25**(5), p 31–32
29. O. Kwon, K.J. Lee, J.K. Lee and K.B. Kang, Modelling for Austenite Evolution and Transformation for Microalloyed Steels, *Microalloying '95*, M. Korchynski, Ed., June 11-14, 1995 (Pittsburgh, PA), ISS-AIME, Warrendale, PA, 1995, p 251–261
30. T.N. Baker, Microalloyed Steels, *Science Progress*, Vol 65, Blackwell Scientific Publisher, Oxford, UK, 1978, p 493–542